

A mathematical model to identify optimal combinations of drug targets for dupilumab poor responders in atopic dermatitis

(Short title: Simulated efficacy for dupilumab poor responders in AD)

Takuya Miyano¹, Alan D Irvine^{2,3} and Reiko J Tanaka^{1*}

1 Department of Bioengineering, Imperial College London, UK

2 Pediatric Dermatology, Children's Health Ireland at Crumlin, Dublin

3 Clinical Medicine, Trinity College Dublin, Dublin, Ireland

*Corresponding author: Reiko J. Tanaka

Department of Bioengineering, Imperial College London

South Kensington Campus, London, SW7 2AZ, UK

+44 20 7594 6374

r.tanaka@imperial.ac.uk

ORCID ID

TM: 0000-0002-1181-6924; ADI: 0000-0002-9048-2044; RJT: 0000-0002-0769-9382

Conflict of Interest statement

ADI has received honorarium for consultancy from AbbVie, Arena Pharmaceuticals, Benevolent AI, Chugai, Dermavant, Genentech, LEO Pharma, Lilly, Menlo Therapeutics, Novartis, Pfizer, Regeneron, Sanofi, and UCB. The other authors declare no competing interests for this work.

Funding information

This work was funded by the British Skin Foundation (005/R/18).

Acknowledgments

We thank Dr Elisa Domínguez-Hüttinger for her insightful comments on our manuscript.

Author Contributions

TM and RJT designed the research and wrote the article. TM performed the research and analyzed the data. TM, ADI and RJT contributed to review and approval of the manuscript.

NOTE: This preprint reports new research that has not been certified by peer review and should not be used to guide clinical practice.

Abstract

Background: Several biologic drugs for atopic dermatitis (AD) have demonstrated good efficacy in clinical trials, but with a substantial proportion of patients being identified as poor responders. This study aims to understand the pathophysiological backgrounds of patient variability in drug response, especially for dupilumab, and to identify promising drug targets in dupilumab poor responders.

Methods: We conducted model-based meta-analysis of recent clinical trials of AD biologics and developed a mathematical model that reproduces reported clinical efficacies for nine biological drugs (dupilumab, lebrikizumab, tralokinumab, secukinumab, fezakinumab, nemolizumab, tezepelumab, GBR 830, and recombinant interferon-gamma) by describing systems-level AD pathogenesis. Using this model, we simulated the clinical efficacy of hypothetical therapies on virtual patients.

Results: IL-13 in the skin was affirmed, by the global sensitivity analysis of our model, as a potential predictive biomarker to stratify dupilumab good responders. The model simulation identified simultaneous inhibition of IL-13 and IL-22 as a promising drug target for dupilumab poor responders, whereas inhibition of either IL-13 or IL-22 alone in these non-responders was ineffective.

Conclusion: We present a mathematical model of AD pathogenesis developed by integration of clinical efficacy data of multiple drugs. This model will serve as a computational platform for model-informed drug development for precision medicine, as it allows evaluation of the effects of new potential drug targets, including combination therapeutics, at an individual patient level and the mechanisms behind patient variability in drug response. Similar mathematical models can be developed for other diseases and drugs, for patient stratification and identification of predictive biomarkers.

KEYWORDS

atopic dermatitis, dupilumab, model-based meta-analysis, poor responders, quantitative systems pharmacology

1. INTRODUCTION

Atopic dermatitis (AD) is the most common inflammatory skin disease, whose incidence is increasing in many areas of the world, especially urbanized areas, with a current worldwide prevalence of 5%-25%¹. Primary symptoms of AD are relapsing pruritus and skin pain, impairing patients' quality of life, for example by sleep disturbance and decreased work productivity especially in moderate-to-severe cases². The pathogenesis of AD involves epidermal barriers abnormalities, dysbiosis and heterogeneous immunological dysregulations^{3,4,5} characterized by a dominant Type 2 immune activation including the T helper (Th) 2 axis and, depending on the lesional stage and ethnicity, varying degrees of upregulation of the Th1, Th17, and Th22 axes. These Th cells produce inflammatory cytokines such as interleukin (IL)-4, IL-13, IL-17A, IL-22, and IL-31, all of which have been identified and investigated as therapeutic targets for AD^{4,5}.

Dupilumab, a monoclonal antibody that inhibits signaling from IL-4 and IL-13 by blocking their common IL-4 receptor subunit α (IL-4R α), was approved as the first and, so far, the only AD-specific biologic in 2017⁶ for its promising efficacy demonstrated in clinical trials. The high efficacy of dupilumab confirmed the clinical validity of IL-4 and IL-13 as therapeutic targets for AD. However, dupilumab treatment was not effective for a sub-population of patients; the responder rates for dupilumab remain 44%-69% for Eczema Area and Severity Index (EASI)-75 (75% reduction in the EASI score^{7, 8}) and 36%-39% for achievement of clear or almost clear skin in Investigator's Global Assessment, respectively^{9, 10}.

A significant percentage of poor responders was also observed for investigational drugs with other mechanisms of action (MoA), even if their clinical efficacy was confirmed for the study population average. It is thus of high clinical importance to identify underlying pathogenesis that causes the patients' variability in responsiveness to each drug, and to investigate whether there are alternative drug targets for those poor responders.

The clinical efficacy of investigational drugs for AD have been evaluated in many clinical trials. Reviewing the combined results from the clinical trials, for example by network meta-analysis¹¹, suggested hypothetical AD pathogenesis described as diagrammatic pathways^{12, 13}. However, such a qualitative framework does not account for patient stratification and for development of drugs that can be effective for poor responders to existing drugs, because underlying mechanisms for the variability in individual patients' responsiveness cannot be evaluated. In addition, a simple correlation analysis between clinical efficacy and biological factors (e.g., transcriptome data)^{14, 15, 16} is not suitable to identify appropriate biomarkers for patient stratification, as it may detect pseudo-correlations rather than the actual causal relationship. Instead, a quantitative model-based framework that describes AD pathogenesis is required to identify biomarkers for patient stratification and to evaluate the clinical efficacy of new hypothetical therapies such as the one that inhibits a combination of cytokines¹⁷.

As a quantitative approach to elucidate disease pathogenesis, quantitative systems

pharmacology (QSP) has been successfully applied to enhance understanding of the pathogenesis of many inflammatory diseases in the context of translational drug development^{18, 19}. QSP uses mathematical models to describe a systems-level understanding of pathogenesis and drug effects by integrating biological and pharmacological knowledge²⁰. For example, the QSP approach has been applied to evaluate the efficacy of approved and experimental drugs in rheumatoid arthritis²¹, the effects of a hypothetical drug on cytokine behaviors in Crohn's disease²², and the relationship between Th1/Th2 responses and exposure levels of lipopolysaccharide in asthma²³. QSP modeling can be leveraged with model-based meta-analysis, which integrates data from different clinical trials with current understanding on disease pathogenesis, to make maximal use of clinical efficacy data of multiple therapies with different MoA²⁴.

In this study, we develop a QSP model that describes the relationship between cytokines and AD pathogenesis using clinical efficacy data of nine approved or investigational biologic drugs: dupilumab, lebrikizumab, tralokinumab, secukinumab, fezakinumab, nemolizumab, tezepelumab, GBR 830, and recombinant interferon-gamma (rIFN γ). We use the model to reveal the pathophysiological backgrounds of dupilumab poor responders and to identify promising drug targets to treat the dupilumab poor responders.

2. METHODS

2.1. Data collection for QSP model to simulate clinical efficacies of AD biologics

We collected reference data from published clinical trials where efficacy of biologic drugs for AD patients were evaluated (detailed in Supplementary Information (SI) Section 1, Figure S1). We considered only the drugs that showed a higher (not necessarily statistically significant) efficacy than placebo in a placebo-controlled double-blinded clinical study (Table 1) and adopted only the highest dose of each drug. For example, we adopted the highest dose, 300 mg weekly, used in the Ph3 study for dupilumab. It allowed us to assess the maximal effects of the MoA and integrate the clinical data from different MoA, rather than investigating the relationship between pharmacokinetics and pharmacodynamics.

We did not consider small molecules because they can affect many cytokines, making it difficult to associate clinical efficacy with a specific cytokine in our model. For example, a Janus kinase (JAK) inhibitor, abrocitinib, was excluded in this study, as JAK inhibitors block signaling of a considerable number of cytokines and growth factors. We used EASI-75 (and its related %improved EASI and mean EASI score) as an efficacy endpoint that was adopted as one of the most common primary endpoints in Ph3 studies^{10,25}. EASI-75 was normalized to compare clinical efficacies of different clinical trials (detailed in SI Section 2).

Reference data for the levels of biological factors, including cytokines, OX40 ligand (OX40L), and T cells in AD skin lesions, were obtained from human skin biopsy data in published observational studies (TABLE S2). We described protein levels of cytokines and OX40L and

count levels of T cells in AD lesion skin by fold change relative to those for healthy subjects or to non-lesional skin of the same AD patients. Our model described skin barrier integrity and infiltrated pathogens as latent state variables, which have no reference data to be compared with simulated values.

2.2. Development of model structure

We developed a mathematical model consisting of 14 ordinary differential equations with 51 parameters to simulate the efficacy of the nine drugs (detailed in SI Section 3). The model structure is based on our previously published mathematical model of AD pathogenesis²⁶. The main feature of the model in this study is its explicit description of the functions of cytokines and OX40L in the skin that have been specifically targeted by the drugs (TABLE 1). Our model also described their related subtypes of Th cells to explicitly represent feedforward and feedback mechanisms (e.g., Th2 secretes IL-4, which promotes T cell differentiation toward Th2). The functional relationships between biological factors in the model were described according to published experimental evidence based on human data.

The model includes the EASI score as a model variable to represent an efficacy endpoint. Some biological factors such as dendritic cells and antimicrobial peptides (AMPs) were not described as model variables, but were taken into consideration as rationale for regulatory processes in our model (e.g., IL-17A decreases infiltrated pathogens via increasing AMPs), to make the model simpler yet interpretable. Our model excluded the targets of the excluded drugs because the contribution of those targets on AD pathogenesis has not been clinically confirmed (e.g., IgE was not considered because anti-IgE antibody omalizumab was excluded).

The model was implemented in Python 3.7.6 (Python Software Foundation).

2.3. Modelling drug effects

All the drugs, except for rIFN γ , inhibit signaling from biological factors by blocking their binding to the receptors by targeting the cytokine itself or its receptor. Effective concentration of the target biological factor in the skin at time t , $c(t)$, was modelled by

$$c(t) = (1 - r_{\text{inhibit}})c^*(t), \quad (1)$$

where $c^*(t)$ is the actual concentration of the target biological factor in the skin at t and r_{inhibit} is the inhibition rate of the target biological factor in the drug treatment. The value of r_{inhibit} was determined using the published data on IC₅₀ and the mean concentration of drugs in the skin²⁷ that was estimated from their concentration in the serum measured in clinical trials (detailed in SI Section 3.4 and TABLE S3).

Administered rIFNg increases the effective amount of IFNg. Effective concentration of IFNg in the skin at t , $c_{\text{IFNg}}(t)$, is modelled by

$$c_{\text{IFNg}}(t) = c_{\text{IFNg}}^*(t) + c_{\text{rIFNg}}, \quad (2)$$

where $c_{\text{IFNg}}^*(t)$ is the actual concentration of IFNg in the skin at t and c_{rIFNg} is the mean concentration of rIFNg in the skin after rIFNg administration. c_{rIFNg} was estimated as 210 based on the pharmacokinetics data of rIFNg²⁸ (detailed in SI Section 3.4).

2.4. Modelling virtual patients and parameter tuning

We represented each virtual patient by a set of values for the 51 model parameters, where each parameter value is taken from log-normal distribution²⁹ (TABLE S4). The probability distribution function, $f(k_n)$, for the n -th parameter, k_n , is defined by

$$f(k_n) = \frac{1}{\sqrt{2\pi}\sigma_n k_n} \exp\left(-\frac{(\ln k_n - \mu_n)^2}{2\sigma_n^2}\right), \quad (3)$$

where μ_n and σ_n are the distribution parameters that represent the mean and the standard deviation of $\ln k_n$, respectively.

We tuned 102 parameters (μ_n and σ_n) that define distributions of the 51 model parameters (detailed in SI Section 4). The 11 parameters, μ_n for elimination rates of the 11 biological factors, were determined using the half-lives measured *in vivo* (serum) in humans (TABLE S5). The remaining 91 parameters were tuned so that the model reproduces the following clinical data;

- The mean and the coefficient of variation of levels of biological factors in observational studies (TABLE S2) and
- The mean EASI scores and EASI-75 when the nine drugs were applied in clinical trials (FIGURE 1).

2.5. Identification of pathophysiological backgrounds that influence %improved EASI of each drug

To identify the pathophysiological backgrounds of virtual patients that influence %improved EASI of each drug most, we conducted a global sensitivity analysis of the model parameters with respect to %improved EASI. We produced 1000 virtual patients by varying the 51 parameters that represent their pathophysiological backgrounds using Latin hypercube sampling (LHS) and computed partial rank correlation coefficient (PRCC)³⁰ between each

parameter and %improved EASI of each drug. LHS is a sampling method to explore the entire space of multidimensional parameters efficiently, and PRCC represents a rank correlation coefficient that is controlled for confounding effects that could lead to detecting pseudo-correlations. The evaluated ranges of $\ln k_n$ were $[\mu_n - \sigma_n, \mu_n + \sigma_n]$. The p -values for the PRCC were adjusted for multiple testing with the Bonferroni procedure, where a significance level of adjusted $p < 0.05$ was used.

2.6. Simulation of clinical efficacy of hypothetical therapy for dupilumab poor responders

We simulated EASI-75 of a hypothetical therapy for virtual dupilumab poor responders. Virtual dupilumab poor responders were the virtual patients who did not achieve the criterion of EASI-75 (more than 75% improvement of EASI score from week 0) at 24 weeks after dosing dupilumab in 1000 virtual patients. The virtual poor responders were treated with a single drug, combinations of two drugs, and a hypothetical therapy that inhibited combinations of two cytokines or all the cytokines considered in the model (inhibiting IL-4, IL-13, IL-17A, IL-22, IL-31, IFNg, and thymic stromal lymphopoietin: TSLP by 99%).

3. RESULTS

3.1. Comparison of clinical efficacy based on normalized EASI

We selected nine biologic drugs with different MoA that have shown clinical efficacy compared to placebo at least at the population average (TABLE 1) and compared the clinical efficacy of the drugs by mean EASI score, %improved EASI, and EASI-75 after normalization (FIGURE 1). Dupilumab and lebrikizumab showed the highest efficacy among the nine drugs, suggesting that their common target, IL-13, has the highest contribution on AD pathogenesis among the drug targets evaluated in this study. All other drugs also achieved a certain efficacy compared to placebo, confirming the clinical relevance of all the targets to AD pathogenesis.

3.2. QSP model of biologics efficacy

We developed a QSP model (FIGURE 2) that describes the MoA for the nine biologic drugs, i.e., regulatory mechanisms between the biological factors and drugs using the published efficacy data from clinical trials.

Our model includes 15 biological factors that are targeted by the nine drugs or that are known to be related to AD pathogenesis (TABLE S2). They are seven cytokines (IL-4, IL-13, IL-17A, IL-22, IL-31, IFNg, and TSLP), OX40L, and four subsets of helper T cell (Th1, Th2, Th17, and Th22) that are the main source of the cytokines, except for TSLP which is secreted from keratinocytes. The model also includes “infiltrated pathogens” and “skin barrier integrity” as the main variables for a model of AD pathogenesis²⁶, and the EASI score as an efficacy

endpoint of each virtual patient. The effects of the drugs were modelled by decreasing or increasing effective concentrations of their target cytokines or OX40L (TABLE S2).

The model contains 51 parameters (e.g., the recovery rate of skin barrier via skin turnover, k_1). We assumed the parameter values, corresponding to the strengths of the regulatory processes, vary between AD patients, so that virtual patients are defined by sets of 51 parameter values. We tuned the distributions of the 51 parameters (TABLE S4) to reproduce the mean and the coefficient of variation of the biological factors in observational studies and mean EASI score and EASI-75 of the drugs (FIGURE 3). The root mean square errors of the mean EASI and EASI-75 between the simulated and reference data were 2.1 (out of 72 = the max EASI) and 7.4%, respectively.

3.3. Influences of pathophysiological backgrounds of virtual patients on clinical efficacy of dupilumab

The variation in the responsiveness to each drug among the patients is considered to be due to the heterogeneity in the pathophysiological backgrounds of the patients. The responder rates could be improved by patient stratification based on biomarkers that reflect pathophysiological backgrounds³¹. Using the QSP model, we can investigate which pathophysiological backgrounds have influence on clinical efficacy of each drug and which cytokines in the skin can be promising biomarkers for patient stratification. We performed a global sensitivity analysis of the model to investigate the influence of the 51 model parameters (that represent pathophysiological backgrounds of the virtual patients) on %improve EASI of each drug using the LHS-PRCC (FIGURE 4).

Ten model parameters had a significant PRCC with the %improved EASI by dupilumab (FIGURE 4). Four out of the ten parameters are IL-13-related (k_{13} , k_{14} , b_2 , and d_{11}), and the remaining six parameters are skin barrier-related parameters (k_1 , k_3 , b_4 , b_6 , d_1 , and d_3) that correspond to placebo effects and baseline severity of skin barrier defects rather than each MoA (SI Section 5). The four IL-13 related parameters (k_{13} , k_{14} , b_2 , and d_{11}) can characterize responders for dupilumab, as virtual patients with higher k_{13} , k_{14} , and b_2 and a lower d_{11} were more responsive to treatment by dupilumab. The parameter, b_2 , describes the influence of IL-13 on skin barrier damage. IL-4-related parameters (k_{11} , k_{12} , b_1 , b_7 , and d_{10}) did not have a significant PRCC with %improved EASI by dupilumab, which inhibits both IL-4 and IL-13 signaling, in consistent with the report that clinical efficacy of dupilumab were not correlated with the baseline level of IL-4 mRNA expression¹⁴.

As three out of the four IL-13 related parameters, k_{13} , k_{14} , and d_{11} , affect the IL-13 baseline level, we hypothesized that baseline levels of some cytokines in the skin could be used as predictive markers of good/poor responders for dupilumab and other drugs. To test this hypothesis, we stratified virtual patients based on their baseline cytokine levels for varying pre-defined threshold values. For the virtual patients whose baseline cytokine level is greater

than the threshold value, we simulated the %improved EASI at week 24 of each drug (FIGURE 5). For dupilumab, EASI-75 was improved for patients with a higher IL-13 baseline level. It is consistent with the results from actual clinical trials of dupilumab, where a higher efficacy was observed in the AD patients with higher baseline messenger RNA (mRNA) levels of IL-13¹⁴.

3.4. Efficacy of existing or hypothetical therapy in dupilumab poor responders

The proportion of poor responders to dupilumab; the actual and simulated percentages of patients who did not achieve EASI-75 at 24 weeks, was 31%¹⁰ and 35% [95% confidence interval (CI) 30.0%-41.9%] respectively (FIGURE 3). However, therapeutic options for the dupilumab poor responders are limited to increasing topical corticosteroids and adding systemic immunosuppressive agents, although the dupilumab poor responders are often resistant to these treatments and require monitoring for adverse effects³².

We hypothesized that the dupilumab poor responders could be responsive to other targeted biologic drugs with different MoA, considering the heterogeneity of AD pathogenesis, and evaluated the potential efficacy of all nine drugs (FIGURE 6a). Every one of the nine drugs failed to show clinical responses in virtual dupilumab poor responders where maximal calculated responder rates, based on EASI-75 at 24 weeks, were only 1.9% [95%CI 0.6%-3.4%] in fezakinumab. These low efficacies imply an upper efficacy ceiling for drugs that target single cytokines to treat dupilumab poor responders.

We then evaluated the potential efficacy of hypothetical therapies that inhibit two cytokines, mimicking a bispecific antibody, for the virtual dupilumab poor responders. Our simulation demonstrated that dosing one additional drug to dupilumab achieved a better efficacy for virtual dupilumab poor responders (FIGURE 6b). The maximal EASI-75 in the virtual dupilumab poor responders (0% achieving EASI-75 at 24 weeks with dupilumab therapy) at 24 weeks was 23.0% [95%CI 18.4%-27.3%] in dupilumab + fezakinumab, implying that inhibition of both IL-13 and IL-22 would be a promising combination for treatment of dupilumab poor responders. Indeed, inhibition of both IL-13 and IL-22 showed the highest clinical responses among all the combinations of two cytokines (FIGURE 6c), with EASI-75 at 24 weeks being 21.6% [95%CI 17.4%-25.5%]. These results are in concordance with a clinically observed negative correlation between the clinical efficacy of dupilumab and the baseline level of IL-22 mRNA expression (not significant, rank correlation coefficient -0.208 with *p*-value of 0.422)¹⁴. The simulation results, in combination with the clinical observation¹⁴, suggest that inhibition of IL-22 in addition to the dupilumab treatment is effective for dupilumab poor responders.

We also confirmed that blocking all targeted cytokines (inhibiting IL-4, IL-13, IL-17A, IL-22, IL-31, IFN γ , and TSLP by 99%) achieved a higher EASI-75 (33.8% [95%CI 28.8%-38.7%], FIGURE 6c). The responder rate did not reach 100% even when all the cytokines were

blocked because some cytokines have not only detrimental but also beneficial effects. For example, IL-17A and IL-22 damage the skin barrier by inhibiting epidermal differentiation (detrimental effects) while they decrease infiltrated pathogens via increasing AMP (beneficial effects). Hence, inhibition of cytokines can partly exacerbate the AD symptoms, suggesting that finding optimal combinations of drugs requires a systems-level investigation.

4. DISCUSSION

4.1. QSP model to simulate biologics efficacy

Several biologic drugs targeting AD pathogenic cytokines have been developed and shown clinical efficacy to some extent in AD patients. Although only one biologic drug, dupilumab, has been currently approved, it is useful to conduct model-based meta-analysis by integrating the results from clinical trials of other biologic drugs, including those that failed to show clinically significant efficacy and those under development, to enhance the understanding of AD pathogenesis and clinical efficacy of drugs with different MoA. In this study, we conducted model-based meta-analysis of clinical trials on the nine biologic drugs for AD (dupilumab, lebrikizumab, tralokinumab, secukinumab, fezakinumab, nemolizumab, and tezepelumab, GBR830, and rIFN γ) that were published by Dec 2020 (FIGURE S1), and developed a QSP model of biologics efficacy in AD patients (FIGURE 2). This QSP model describes dynamic relationships between biological factors and clinical efficacies by integrating knowledge obtained from experiments using human samples and clinical trials of multiple drugs. The model reproduced the clinical efficacies of the biologic drugs observed in clinical trials and baseline levels of biological factors (e.g., cytokines) in the skin from published studies (FIGURE 3).

4.2. Comparison of clinical efficacies of biologics

Comparison of clinical efficacies (FIGURE 1) demonstrated that dupilumab and lebrikizumab showed the highest efficacy among the nine drugs investigated in this study, suggesting that their common target, IL-13, is the most crucial target to improve AD severity scores. The comparable efficacy between dupilumab (inhibiting both IL-4 and IL-13) and lebrikizumab (inhibiting IL-13 only) may suggest inhibition of IL-4 signaling has a minor contribution on the efficacy of dupilumab. Another anti-IL-13 antibody, tralokinumab, showed a significantly lower clinical efficacy than lebrikizumab. Lebrikizumab inhibits binding of IL-13 to IL-13R α 1 only, while tralokinumab inhibits binding to both IL-13R α 1 and IL-13R α 2. IL-13R α 1 forms a heterodimeric receptor with IL-4R α and is related to the effects of IL-13 signaling in AD pathogenesis while IL-13R α 2 is a decoy receptor to decrease IL-13 signaling via IL-13R α 1. Hence, tralokinumab not only inhibits IL-13 signaling via IL-13R α 1 but also enhances IL-13 signaling via inhibition of IL-13 binding to IL-13R α 2³³. In our simulation, effective inhibition of IL-13 signaling by tralokinumab was estimated 44% of lebrikizumab ($e_{a2} = 0.44$). The

difference in the efficacy between lebrikizumab and tralokinumab may come from different mechanisms for IL-13 inhibition, dosing regimens, or trial design.

4.3. Pathophysiological backgrounds of dupilumab poor responders

This study presents a QSP-based approach to identify potential predictive biomarkers of clinical efficacy through mechanistic model-based simulation. We used the developed model to explore pathophysiological backgrounds of dupilumab poor responders. Our simulation demonstrated that the higher responder rates for dupilumab are expected in patients with the higher baseline level of IL-13 in the skin (FIGURES 4 and 5). Although it also showed baseline levels of other cytokines (e.g., IFN γ) in the skin influence responder rates, these influences may be due to a pseudo-correlation of the cytokines with clinical efficacy because the parameters related to those cytokines were not detected as important in the global sensitivity analysis, which evaluates the “causative” influence of the parameters on efficacy. The cytokines detected due to the pseudo-correlation should not be used as predictive biomarkers for patient stratification, because such pseudo-correlations may have low reproducibility. Hence, our simulations suggest that the baseline level of IL-13 in the skin would be more suitable than other cytokines to be used as a biomarker for patient stratification in dupilumab treatment.

4.4. Simulated efficacy of hypothetical therapy in dupilumab poor responders

We also used the model to investigate alternative therapeutic options for virtual dupilumab poor responders. Our simulation results suggested inhibition of a single cytokine would be insufficient to achieve clinical response in virtual dupilumab poor responders, whereas inhibition of multiple cytokines could achieve clinical response (FIGURE 6a,b). Especially, IL-13 and IL-22 were identified to be the best combination to treat virtual dupilumab poor responders (FIGURE 6c). Inhibition of two cytokines can be realized by a bispecific antibody as well as combination of two antibodies.

Our simulated hypothetical therapy that inhibits all the cytokines in this model (IL-4, IL-13, IL-17A, IL-22, IL-31, IFN γ , and TSLP) showed higher clinical efficacy than inhibiting single and a combination of two cytokines (FIGURE 6c). These results suggest that inhibiting multiple cytokines can exert higher efficacy than biologic drugs targeting only one or two cytokines. In fact, the approach to inhibit signaling of multiple cytokines has been already realized by JAK inhibitors. For instance, abrocitinib blocks JAK1, which is an intracellular tyrosine kinase linked to intracellular domains of many cytokine receptors, including IL-4, IL-13, IL-22, IL-31, IFN γ , and TSLP. Abrocitinib showed comparable efficacy with dupilumab¹¹, but there were still a significant percentage of poor responders. One of the reasons why even multiple cytokine inhibition cannot achieve clinical response in all AD patients is that inhibition of cytokines can deteriorate AD symptoms because some cytokines have both detrimental and beneficial effects in AD pathogenesis and the contributions of each cytokine on AD

pathogenesis would vary among the AD patients. Hence, appropriate drugs would vary according to the pathophysiological backgrounds of the patients. Patient stratification may be beneficial not only for biologic drugs but also for the drugs that target multiple cytokines.

4.5. Limitation of this study using the model

We used clinical efficacy results of the biologic drugs as the reference data to tune the model parameters. We adopted Ph2 as well as Ph3 studies to make a maximal use of available clinical data (TABLE 1). However, the results from Ph2 studies with a rather small number of patients need to be confirmed with those from Ph3 studies with a larger number of patients. Our model assumptions include that virtual patients were generated from single modal distributions of the model parameters. There could be a multimodal distribution due to the genetic backgrounds or other demographic variances in a real population of AD patients. For the practical purposes of generating this model we assumed the %improved EASI was comparable across clinical trials. We know that outcome measures may be influenced by the concomitant use of topical corticosteroids and the statistical methods used to adjust for or censor topical corticosteroid use and to impute missing data. The model will need to be updated according to availability of the reference data and assumptions if these are changed as new data emerge.

4.6. Prospects for model-informed drug development

The proposed model could be further expanded for future development of new drugs for AD, by including new drug targets and pharmacokinetics and pharmacodynamics profiles of new drugs. The expanded model will be a useful tool to computationally evaluate potential clinical efficacies of new drug candidates, to identify biomarkers for patient stratification, to clarify the difference from existing drugs (e.g., showing significant efficacy in dupilumab poor responders), and to design optimal doses with considering variations in pathophysiological backgrounds. The model contributes to a systems-level understanding of AD pathogenesis and the drug effects and to evaluate the effects of new potential drug targets by computational simulation. This could serve as model-informed drug development³⁴ for precision medicine. The code of the QSP model is available at https://github.com/Tanaka-Group/AD_QSP_model.

TABLE 1 Drugs considered in this study

Drugs	Targets	Dose regimen (highest dose)	Available endpoints	efficacy	#patients in placebo/drug arm (Phase)
Dupilumab ¹⁰ (anti-IL-4 receptor subunit α antibody)	IL-4 and IL-13	300 mg qw, s.c. +TCS	EASI-75, %improved EASI %improved SCORAD		264/270 (Ph3)
Lebrikizumab ⁴⁰ (anti-IL-13 antibody)	IL-13	250 mg q2w, s.c. +TCS	EASI-75, %improved EASI		52/75 (Ph2)
Tralokinumab ³⁹ (anti-IL-13 antibody)	IL-13	300 mg q2w, s.c. +TCS	EASI-75 %improved EASI		126/252 (Ph3)
Secukinumab ¹⁶ (anti-IL-17A antibody)	IL-17A	300 mg qw for 4 weeks, followed by 300 mg q4w	%improved EASI %improved SCORAD		14/27 (Ph2)
Fezakinumab ³⁶ (anti-IL-22 antibody)	IL-22	600 mg at day 0, followed by 300 mg q2w, i.v.	%improved SCORAD [†]		20/40 (Ph2)
Nemolizumab ³⁵ (anti-IL-31 receptor subunit α antibody)	IL-31	60 mg q4w, s.c.	EASI-75, %improved EASI		72/143 (Ph3)
Tezepelumab ³⁷ (anti-TSLP antibody)	TSLP	280 mg q2w, s.c. +TCS	EASI-75, %improved EASI %improved SCORAD		56/55 (Ph2)
GBR 830 ³⁸ (anti-OX40L antibody)	OX40L	10 mg/kg q4w, i.v.	%improved EASI		16/46 (Ph2)
rIFNg ⁴¹	IFNg	50 ug/m2 qd, s.c. +TCS	% improved AD scores [‡]		43/40 (Ph2)

†: %improved EASI was estimated from %improved SCORAD using a regression curve (FIGURE S2), ‡: the mean value of the %improved AD scores were regarded as %improved EASI because the evaluated signs were same as those for EASI (erythema, induration, excoriations, and lichenification). When there were multiple clinical studies per drug, we adopted the clinical study of combination therapy with topical corticosteroids, which is more reflective of the likely clinical use compared with monotherapy, and studies with the largest number of patients.

Abbreviations: qw, every week; q2w, every 2 weeks; q4w, every 4 weeks; qd, every day; s.c., subcutaneous administration; i.v., intravenous administration; +TCS, concomitant use of topical corticosteroids.

References

1. Deckers IA, McLean S, Linssen S, Mommers M, van Schayck CP, Sheikh A. Investigating international time trends in the incidence and prevalence of atopic eczema 1990-2010: a systematic review of epidemiological studies. *PLoS One*. 2012;7:e39803
2. Simpson EL, Bieber T, Eckert L, Wu R, Ardeleanu M, Graham NM, Pirozzi G, Mastey V. Patient burden of moderate to severe atopic dermatitis (AD): Insights from a phase 2b clinical trial of dupilumab in adults. *J Am Acad Dermatol*. 2016;74:491-8
3. Czarnecki T, He H, Krueger JG, Guttman-Yassky E. Atopic dermatitis endotypes and implications for targeted therapeutics. *J Allergy Clin Immunol*. 2019;143:1-11
4. Langan SM, Irvine AD, Weidinger S. Atopic dermatitis. *Lancet*. 2020;396:345-360.
5. Weidinger S, Beck LA, Bieber T, Kabashima K, Irvine AD. Atopic dermatitis. *Nat Rev Dis Primers*. 2018;4:1
6. Shirley M. Dupilumab: First Global Approval. *Drugs*. 2017;77:1115-1121
7. Hanifin JM, Thurston M, Omoto M, Cherill R, Tofte SJ, Graeber M. The eczema area and severity index (EASI): assessment of reliability in atopic dermatitis. EASI Evaluator Group. *Exp Dermatol*. 2001;10:11-18
8. Schram ME, Spuls PI, Leeflang MM, Lindeboom R, Bos JD, Schmitt J. EASI, (objective) SCORAD and POEM for atopic eczema: responsiveness and minimal clinically important difference. *Allergy*. 2012;67:99-106
9. Simpson EL, Bieber T, Guttman-Yassky E, et al. Two Phase 3 Trials of Dupilumab versus Placebo in Atopic Dermatitis. *N Engl J Med*. 2016;375:2335-2348
10. Blauvelt A, de Bruin-Weller M, Gooderham M, et al. Long-term management of moderate-to-severe atopic dermatitis with dupilumab and concomitant topical corticosteroids (LIBERTY AD CHRONOS): a 1-year, randomised, double-blinded, placebo-controlled, phase 3 trial. *Lancet*. 2017;389:2287-2303
11. Drucker AM, Ellis AG, Bohdanowicz M, et al. Systemic Immunomodulatory Treatments for Patients With Atopic Dermatitis: A Systematic Review and Network Meta-analysis. *JAMA Dermatol*. 2020;156:659-667
12. Renert-Yuval Y, Guttman-Yassky E. New treatments for atopic dermatitis targeting beyond IL-4/IL-13 cytokines. *Ann Allergy Asthma Immunol*. 2020;124:28-35
13. Noda S, Krueger JG, Guttman-Yassky E. The translational revolution and use of biologics in patients with inflammatory skin diseases. *J Allergy Clin Immunol*. 2015;135:324-336
14. Guttman-Yassky E, Bissonnette R, Ungar B, et al. Dupilumab progressively improves systemic and cutaneous abnormalities in patients with atopic dermatitis. *J Allergy Clin Immunol*. 2019;143:155-172
15. Brunner PM, Pavel AB, Khattri S, et al. Baseline IL-22 expression in patients with atopic dermatitis stratifies tissue responses to fezakinumab. *J Allergy Clin Immunol*.

2019;143:142-154

16. Ungar B, Pavel AB, Li R, et al. Phase 2 randomized, double-blind study of IL-17 targeting with secukinumab in atopic dermatitis. *J Allergy Clin Immunol*. 2021;147:394-397
17. Paternoster L, Savenije OEM, Heron J, et al. Identification of atopic dermatitis subgroups in children from 2 longitudinal birth cohorts. *J Allergy Clin Immunol*. 2018;141:964-971
18. Knight-Schrijver VR, Chelliah V, Cucurull-Sanchez L, Le Novère N. The promises of quantitative systems pharmacology modelling for drug development. *Comput Struct Biotechnol J*. 2016;14:363-370
19. Nijsen MJMA, Wu F, Bansal L, et al. Preclinical QSP Modeling in the Pharmaceutical Industry: An IQ Consortium Survey Examining the Current Landscape. *CPT Pharmacometrics Syst Pharmacol*. 2018;7:135-146
20. Schoeberl B. Quantitative Systems Pharmacology models as a key to translational medicine. *Curr Opin Syst Biol* 2019;16:25–31
21. Moise N, Friedman A. Rheumatoid arthritis - a mathematical model. *J Theor Biol*. 2019;461:17-33
22. Balbas-Martinez V, Asin-Prieto E, Parra-Guillen ZP, Troconiz IF. A Quantitative Systems Pharmacology Model for the Key Interleukins Involved in Crohn's Disease. *J Pharmacol Exp Ther*. 2020;372:299-307
23. Kim Y, Lee S, Kim YS, et al. Regulation of Th1/Th2 cells in asthma development: a mathematical model. *Math Biosci Eng*. 2013;10(4):1095-1133
24. Gibbs JP, Menon R, Kasichayanula S. Bedside to Bench: Integrating Quantitative Clinical Pharmacology and Reverse Translation to Optimize Drug Development. *Clin Pharmacol Ther*. 2018;103(2):196-198
25. Silverberg JI, Simpson EL, Thyssen JP, et al. Efficacy and Safety of Abrocitinib in Patients With Moderate-to-Severe Atopic Dermatitis: A Randomized Clinical Trial. *JAMA Dermatol*. 2020;156:863-873
26. Domínguez-Hüttinger E, Christodoulides P, Miyauchi K, et al. Mathematical modeling of atopic dermatitis reveals "double-switch" mechanisms underlying 4 common disease phenotypes. *J Allergy Clin Immunol*. 2017;139:1861-1872.e7
27. Vazquez ML, Kaila N, Strohbach JW, et al. Identification of N-{cis-3-[Methyl(7H-pyrrolo[2,3-d]pyrimidin-4-yl)amino]cyclobutyl}propane-1-sulfonamide (PF-04965842): A Selective JAK1 Clinical Candidate for the Treatment of Autoimmune Diseases. *J Med Chem*. 2018;61:1130-1152
28. Satake I, Tari K, Nakagomi K, Ozawa K. Feasibility and pharmacokinetics of continuous subcutaneous infusion of low-dose interferon-gamma: a pilot study. *Jpn J Clin Oncol*. 1993;23:356-362
29. Limpert E, Stahel WA, Abbt M. Log-normal distributions across the sciences: keys and

clues: on the charms of statistics, and how mechanical models resembling gambling machines offer a link to a handy way to characterize log-normal distributions, which can provide deeper insight into variability and probability—normal or log-normal: that is the question. *BioScience*. 2001;51:341-352

30. Marino S, Hogue IB, Ray CJ, Kirschner DE. A methodology for performing global uncertainty and sensitivity analysis in systems biology. *J Theor Biol*. 2008;254:178-196
31. Cianferoni A, Annesi-Maesano I. Precision medicine in atopic diseases. *Curr Opin Allergy Clin Immunol*. 2019;19:654-664
32. Hendricks AJ, Lio PA, Shi VY. Management Recommendations for Dupilumab Partial and Non-durable Responders in Atopic Dermatitis. *Am J Clin Dermatol*. 2019;20:565-569
33. Popovic B, Breed J, Rees DG, et al. Structural Characterisation Reveals Mechanism of IL-13-Neutralising Monoclonal Antibody Tralokinumab as Inhibition of Binding to IL-13R α 1 and IL-13R α 2. *J Mol Biol*. 2017;429:208-219
34. EFPIA MID3 Workgroup, Marshall SF, Burghaus R, et al. Good Practices in Model-Informed Drug Discovery and Development: Practice, Application, and Documentation. *CPT Pharmacometrics Syst Pharmacol*. 2016;5:93-122
35. Kabashima K, Matsumura T, Komazaki H, Kawashima M; Nemolizumab-JP01 Study Group. Trial of Nemolizumab and Topical Agents for Atopic Dermatitis with Pruritus. *N Engl J Med*. 2020;383:141-150
36. Guttman-Yassky E, Brunner PM, Neumann AU, et al. Efficacy and safety of fezakinumab (an IL-22 monoclonal antibody) in adults with moderate-to-severe atopic dermatitis inadequately controlled by conventional treatments: A randomized, double-blind, phase 2a trial. *J Am Acad Dermatol*. 2018;78:872-881.e6
37. Simpson EL, Parnes JR, She D, et al. Tezepelumab, an anti-thymic stromal lymphopoietin monoclonal antibody, in the treatment of moderate to severe atopic dermatitis: A randomized phase 2a clinical trial. *J Am Acad Dermatol*. 2019;80:1013-1021
38. Guttman-Yassky E, Pavel AB, Zhou L, et al. GBR 830, an anti-OX40, improves skin gene signatures and clinical scores in patients with atopic dermatitis. *J Allergy Clin Immunol*. 2019;144:482-493.e7
39. Silverberg JI, Toth D, Bieber T, et al. Tralokinumab plus topical corticosteroids for the treatment of moderate-to-severe atopic dermatitis: results from the double-blind, randomized, multicentre, placebo-controlled phase III ECZTRA 3 trial [published online ahead of print, 2020 Sep 30]. *Br J Dermatol*. 2020;10.1111/bjd.19573.
40. Guttman-Yassky E, Blauvelt A, Eichenfield LF, et al. Efficacy and Safety of Lebrikizumab, a High-Affinity Interleukin 13 Inhibitor, in Adults With Moderate to Severe Atopic Dermatitis: A Phase 2b Randomized Clinical Trial. *JAMA Dermatol*. 2020;156:411-420
41. Hanifin JM, Schneider LC, Leung DY, et al. Recombinant interferon gamma therapy for atopic dermatitis. *J Am Acad Dermatol*. 1993;28:189-197

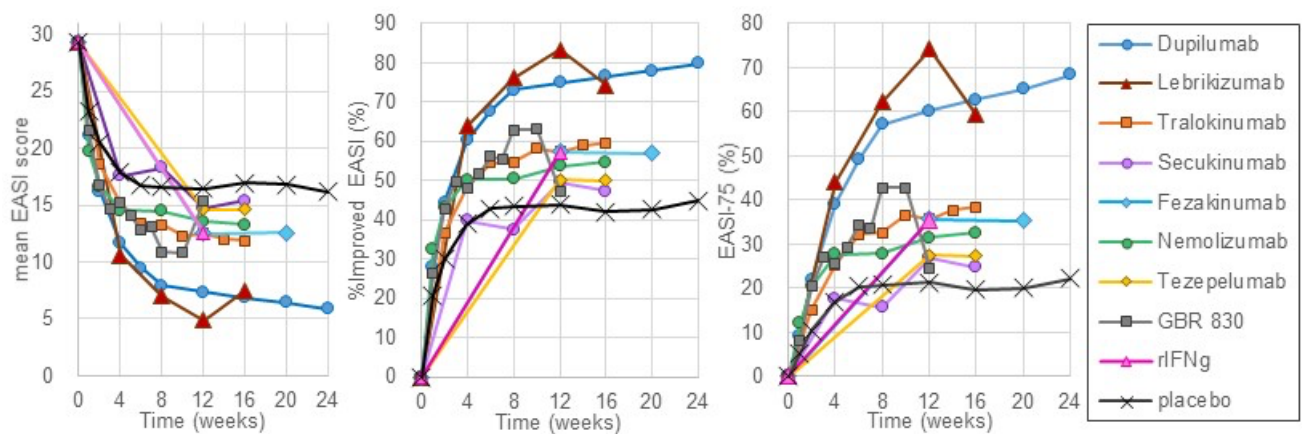


FIGURE 1 Reference data collected from published clinical trials. Normalized mean EASI score, %improved EASI, and EASI-75 obtained by results of clinical trials for nine drugs (dupilumab, lebrikizumab, tralokinumab, GBR 830, fezakinumab, rIFNg, tezepelumab, nemolizumab, secukinumab) and placebo.

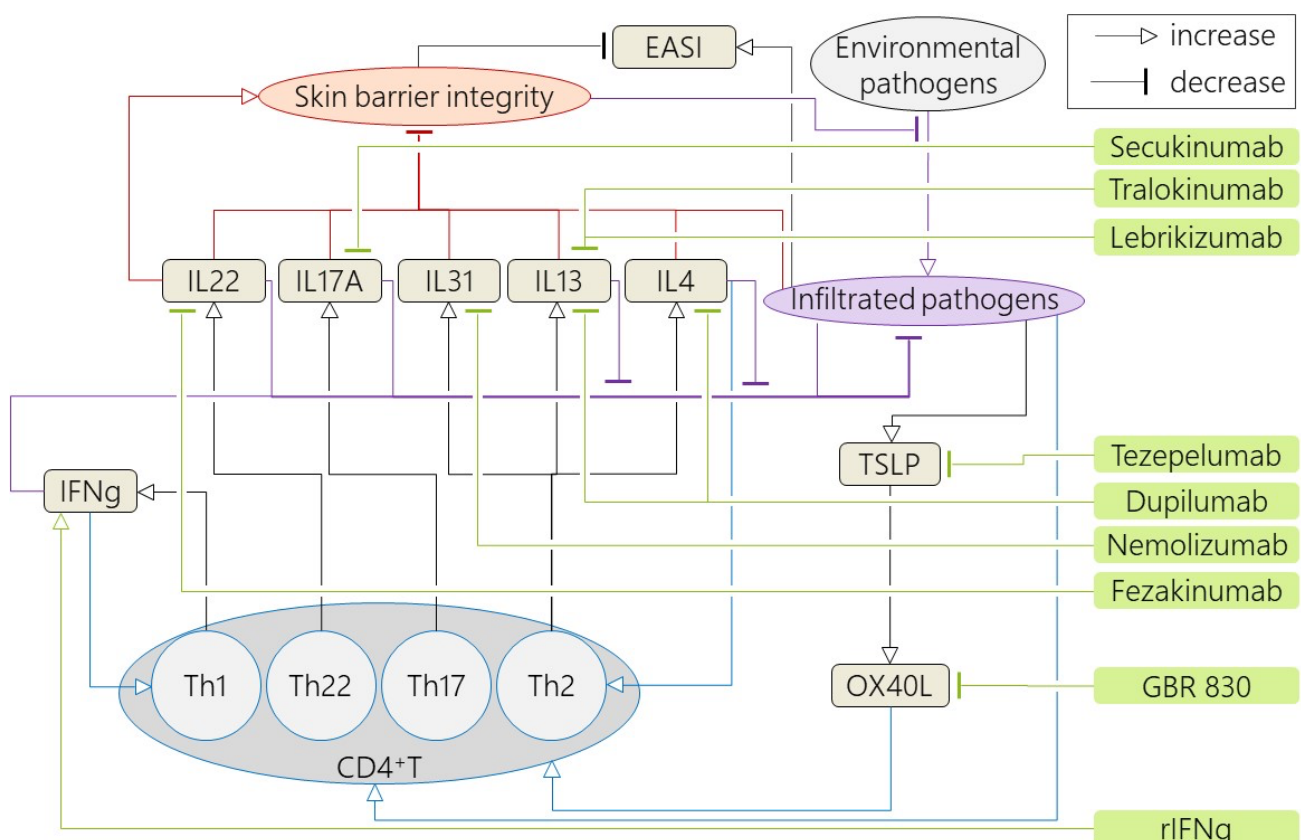


FIGURE 2 Overview of the proposed mathematical model. Details of the model, including ordinary differential equations for dynamics of biological factors and rationale for the functional relationships between biological factors, are described in SI Section 3.

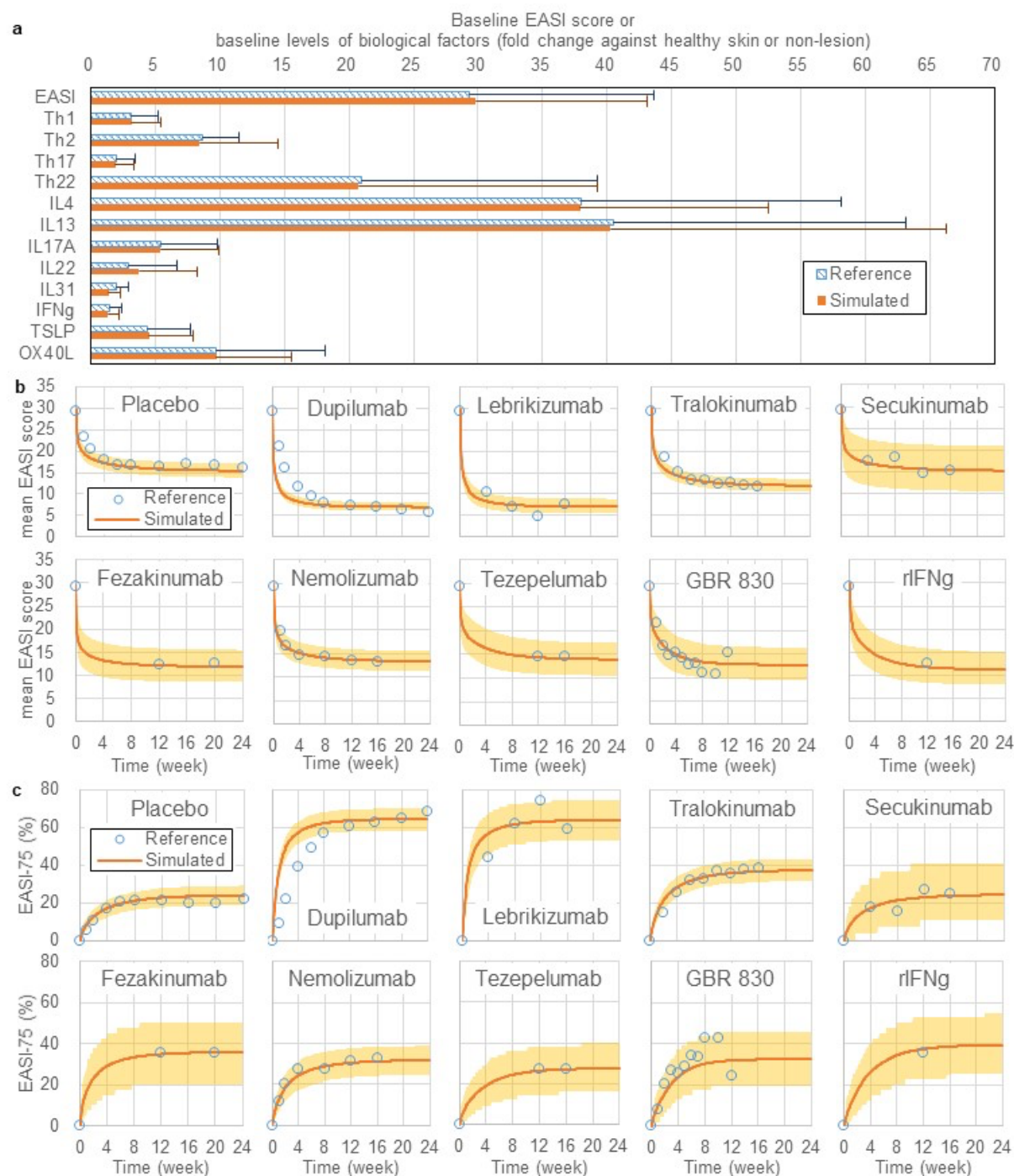


FIGURE 3 Simulated and reference data of (a) baseline levels of biological factors, (b) mean EASI score, and (c) EASI-75. (a) Reference data (striped bars) are the measured values of the biological factors in the observational studies. Simulated data (filled bars) are the simulated values of the biological factors at the steady-state (after 1000 weeks) using 1000 virtual patients. Error bars are standard deviations. (b and c) Reference data (unfilled circles) are mean EASI scores (b) and EASI-75 (c) after treatment of each investigational drug. Simulated data (lines and 95% CI) describe mean EASI score (b) and EASI-75 (c) of 1000 simulations for the same number of virtual patients as for the clinical trials.

Parameters		%improved EASI at week 24									
		Placebo	Dupilumab	Lebrikizumab	Tralokinumab	Secukinumab	Fezakinumab	Nemolizumab	Tezepelumab	GBR 830	rlFNg
Recovery rate of skin barrier integrity via skin turnover	k1	-0.5	-0.6	-0.6	-0.5	-0.5	-0.6	-0.5	-0.5	-0.5	-0.6
Recovery rate of skin barrier integrity via IL-22	k2	0.1	0.1	0.1	0.1	0.1	0.1	0.1	0.1	0.1	0.1
Recovery rate of skin barrier integrity via placebo effects	k3	0.7	0.6	0.6	0.7	0.7	0.7	0.7	0.7	0.7	0.7
Rate of pathogen infiltration	k4	0.0	0.0	0.0	0.0	0.0	0.0	0.0	0.0	0.0	0.0
Rate of differentiation of naïve T cells to Th1	k5	0.0	0.0	0.0	0.0	0.0	0.0	0.0	0.0	0.0	0.0
Rate of differentiation of naïve T cells to Th2	k6	0.0	0.0	0.0	0.0	0.0	0.0	0.0	0.0	0.0	0.0
Rate of differentiation of naïve T cells to Th17	k7	0.0	0.0	0.0	0.0	0.0	0.0	0.0	0.0	0.0	0.0
Rate of differentiation of naïve T cells to Th22	k8	0.1	0.0	0.0	0.0	0.1	0.1	0.1	0.0	0.0	0.0
Strength of polarization for Th1 differentiation	k9	0.0	0.0	0.0	0.0	0.0	0.0	0.0	0.0	0.0	0.2
Strength of polarization for Th2 differentiation	k10	0.0	0.0	0.0	0.0	0.0	0.0	0.0	0.0	0.0	0.0
IL-4 secretion rate via Th2	k11	0.0	0.0	0.0	0.0	0.0	0.0	0.0	0.0	0.0	0.0
IL-4 secretion rate via other pathways	k12	0.0	0.0	0.0	0.0	0.0	0.0	0.0	0.0	0.0	0.0
IL-13 secretion rate via Th2	k13	0.0	0.2	0.2	0.0	0.0	0.1	0.1	0.0	0.0	0.0
IL-13 secretion rate via other pathways	k14	0.1	0.3	0.3	0.0	0.0	0.1	0.1	0.0	0.0	0.0
IL-17A secretion rate via Th17	k15	0.0	0.0	0.0	0.0	0.0	0.0	0.0	0.0	0.0	0.0
IL-17A secretion rate via other factors	k16	0.0	0.0	0.0	0.0	0.0	0.0	0.0	0.0	0.0	0.0
IL-22 secretion rate via Th22	k17	0.0	0.0	0.0	0.0	0.0	0.0	0.0	0.0	0.0	0.0
IL-22 secretion rate via other factors	k18	0.0	0.0	0.0	0.0	0.0	0.0	0.0	0.0	0.0	0.0
IL-31 secretion rate via Th2	k19	0.1	0.0	0.0	0.0	0.0	0.0	0.0	0.0	0.0	0.0
IL-31 secretion rate via other factors	k20	0.0	0.0	0.0	0.0	0.0	0.0	0.0	0.0	0.0	0.0
IFN γ secretion rate via Th1	k21	0.0	0.0	0.0	0.0	0.0	0.0	0.0	0.0	0.0	0.0
IFN γ secretion rate via other factors	k22	0.0	0.0	0.0	0.0	0.0	0.0	0.0	0.0	0.0	0.0
TSLP secretion rate via infiltrated pathogens	k23	0.0	0.0	0.0	0.0	0.0	0.0	0.0	0.0	0.0	0.0
TSLP secretion rate via other factors	k24	0.0	0.0	0.0	0.0	0.0	0.0	0.0	0.0	0.0	0.0
OX40L expression rates via TSLP	k25	0.0	0.0	0.0	0.0	0.0	0.0	0.0	0.0	0.0	0.0
OX40L expression rates via other factors	k26	0.0	0.0	0.0	0.0	0.0	0.1	0.1	0.0	0.0	0.0
Inhibitory strength for recovery of skin barrier via IL-4	b1	0.0	0.0	0.0	0.0	0.0	0.0	0.0	0.0	0.0	0.0
Inhibitory strength for recovery of skin barrier via IL-13	b2	0.0	0.6	0.6	0.3	0.1	0.2	0.1	0.0	0.0	0.2
Inhibitory strength for recovery of skin barrier via IL-17	b3	0.0	0.0	0.0	0.0	0.0	0.0	0.0	0.0	0.0	0.0
Inhibitory strength for recovery of skin barrier via IL-22	b4	0.0	0.2	0.2	0.0	0.1	0.3	0.1	0.0	0.0	0.2
Inhibitory strength for recovery of skin barrier via IL-31	b5	0.0	0.0	0.0	0.0	0.0	0.0	0.1	0.0	0.0	0.0
inhibitory strength for pathogens infiltration via skin barrier	b6	0.2	0.2	0.2	0.2	0.2	0.2	0.2	0.2	0.2	0.2
Inhibitory strength for elimination of infiltrated pathogens via IL-4	b7	0.0	0.0	0.0	0.0	0.0	0.0	0.0	0.0	0.0	0.0
Inhibitory strength for elimination of infiltrated pathogens via IL-13	b8	0.1	0.0	0.0	0.0	0.0	0.0	0.1	0.0	0.0	0.0
Inhibitory strength for T cells elimination by OX40L	b9	0.1	0.1	0.1	0.0	0.0	0.1	0.1	0.0	0.0	0.0
Degradation rate of skin barrier via skin turnover	d1	0.0	0.3	0.3	0.1	0.1	0.3	0.0	0.0	0.0	0.2
Degradation rate of skin barrier via IL-31	d2	0.1	0.1	0.1	0.1	0.1	0.1	0.1	0.0	0.0	0.0
Degradation rate of skin barrier via infiltrated pathogens	d3	0.0	0.3	0.3	0.1	0.0	0.2	0.0	0.0	0.0	0.2
Elimination rate of infiltrated pathogens via infiltrated pathogens themselves	d4	0.0	0.1	0.1	0.0	0.0	0.1	0.0	0.0	0.0	0.0
Elimination rate of infiltrated pathogens via IL-17A	d5	0.0	0.0	0.0	0.0	0.0	0.0	0.0	0.0	0.0	0.0
Elimination rate of infiltrated pathogens via IL-22	d6	0.0	0.0	0.0	0.0	0.0	0.0	0.0	0.0	0.0	0.0
Elimination rate of infiltrated pathogens via IFN γ	d7	0.1	0.1	0.1	0.0	0.0	0.1	0.1	0.0	0.0	0.0
Elimination rate of infiltrated pathogens via skin turnover	d8	0.0	0.0	0.0	0.0	0.0	0.0	0.0	0.0	0.0	0.0
T cell elimination rate	d9	0.1	0.1	0.1	0.0	0.0	0.1	0.1	0.0	0.0	0.0
Elimination rates for IL-4	d10	0.0	0.0	0.0	0.0	0.0	0.0	0.0	0.0	0.0	0.0
Elimination rates for IL-13	d11	0.1	-0.2	-0.2	0.0	0.0	0.1	0.1	0.0	0.0	0.0
Elimination rates for IL-17A	d12	0.0	0.0	0.0	0.0	0.0	0.0	0.0	0.0	0.0	0.0
Elimination rates for IL-22	d13	0.0	0.1	0.1	0.0	0.0	-0.2	0.0	0.0	0.0	0.0
Elimination rates for IL-31	d14	0.0	0.0	0.0	0.0	0.0	0.0	0.0	0.0	0.0	0.0
Elimination rates for IFN γ	d15	0.0	0.1	0.1	0.0	0.0	0.0	0.0	0.0	0.0	0.0
Elimination rates for TSLP	d16	0.0	0.0	0.0	0.0	0.0	0.0	0.0	0.0	0.0	0.0
Elimination rates for OX40L	d17	0.1	0.0	0.0	0.0	0.0	0.0	0.0	0.0	0.0	0.0

FIGURE 4 Effects of model parameters on %improved EASI by drug treatment. Values are PRCC (partial rank correlation coefficient) between each parameter and %improved EASI at 24 weeks after drug treatment in 1000 virtual patients generated by independently sampling 51 parameter values according to LHS (Latin hypercube sampling). Open and crossed cells are statistically significant and not significant PRCC (absolute value >0.1 with adjusted p -values <0.05), respectively. Positive PRCC means that virtual patients with a higher value of the parameter achieve a higher %improve EASI by the drug treatment (e.g., k_3). Negative PRCC means that virtual patients with a lower value of the parameter achieve a higher %improve EASI by the drug treatment (e.g., k_1).

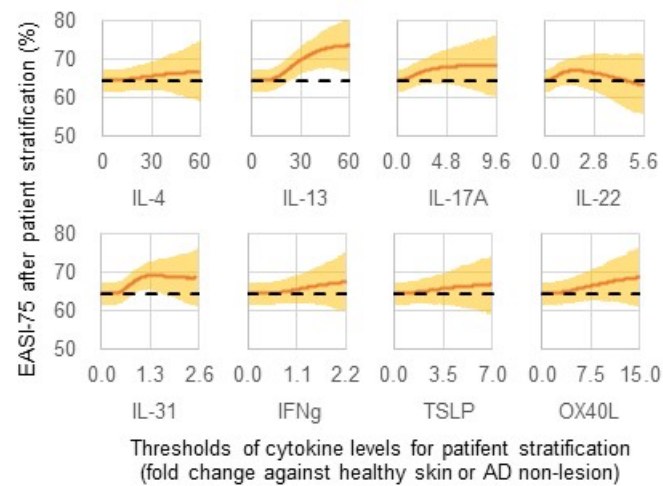


FIGURE 5 Simulated EASI-75 at 24 weeks in dupilumab treatment after patient stratification with different thresholds of cytokine baseline levels. The y-axis displays EASI-75 (responder rates) at 24 weeks in dupilumab treatment in the stratified virtual patients whose baseline level of each cytokine in the skin (before dupilumab treatment) was greater than the threshold (x-axis). The number of stratified virtual patients decreases with an increasing threshold, while the threshold of zero includes all the virtual patients and the maximum threshold investigated includes at least 10% of 1000 virtual patients. Line and shaded area are the mean value and 95% CI of 1000 simulations, respectively. The higher EASI-75 achieved with patient stratification (compared to without stratification with the threshold zero: dashed line) suggests a success in stratifying good responders.

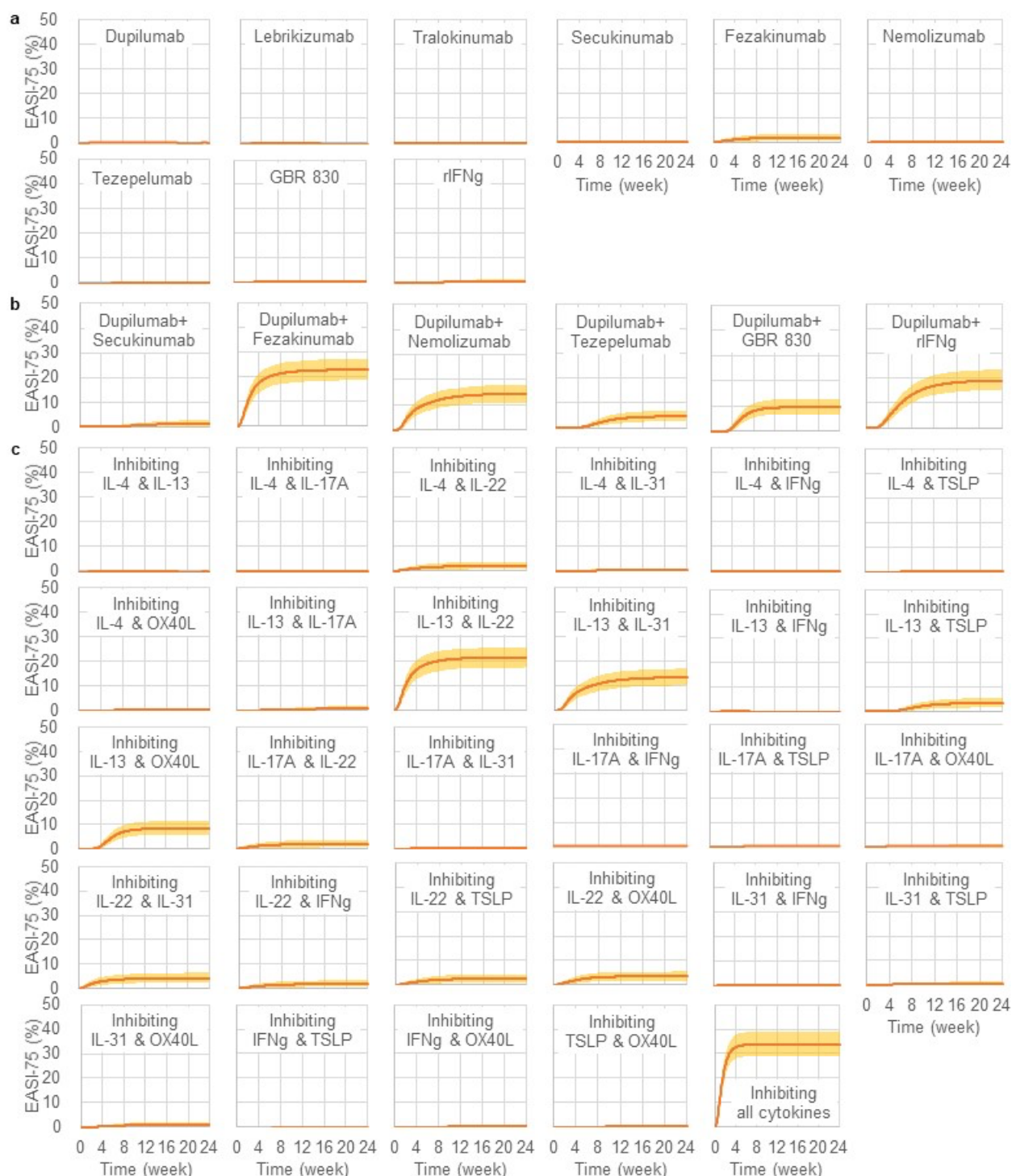


FIGURE 6 Simulated EASI-75 in virtual dupilumab poor-responders. The virtual dupilumab poor-responders were treated with (a) a single drug, (b) a combination of two drugs, and (c) blocking a combination of two cytokines or all the cytokines (inhibiting IL-4, IL-13, IL-17A, IL-22, IL-31, IFNg, and TSLP by 99%). Virtual dupilumab poor responders were 356 (with 95% CI 300-419) virtual patients who did not achieve the criterion of EASI-75 at 24 weeks after dosing dupilumab in 1000 virtual patients. Lines and shaded areas are the mean values and 95% CI of 1000 simulations, respectively.